ISSN 1063-7737, Astronomy Letters, 2015, Vol. 41, Nos. 1–2, pp. 14–22. © Pleiades Publishing, Inc., 2015.
Original Russian Text © V.G. Klochkova, V.E. Panchuk, N.S. Tavolzhanskaya, 2015, published in Pis'ma v Astronomicheskiĭ Zhurnal, 2015, Vol. 41, Nos. 1–2, pp. 17–26.

Peculiarities of the Atmosphere and Envelope of a Post-AGB Star, the Optical Counterpart of IRAS 23304+6347

V. G. Klochkova*, V. E. Panchuk, and N. S. Tavolzhanskaya

Special Astrophysical Observatory, Russian Academy of Sciences, Nizhnii Arkhyz, Karachai-Cherkessian Republic, 369167 Russia

Received September 2, 2014

Abstract—Based on our high-spectral-resolution observations performed with the echelle spectrograph of the 6-m telescope, we have studied the peculiarities of the spectrum and the velocity field in the atmosphere and envelope of the optical counterpart of the infrared source IRAS 23304+6347. We have reached the conclusion about the absence of significant variations in the radial velocity V_r inferred from atmospheric absorptions and about its coincidence with the systemic velocity deduced from radio data. The envelope expansion velocity $V_{\rm exp} = 15.5$ km s^{-1} has been determined from the positions of rotational lines of the C_2 Swan (0; 0) band. A complex emission–absorption profile of the Swan (0; 1) 5635 Å band has been recorded. Our analysis of the multicomponent Na I D doublet line profile has revealed interstellar components with velocities $V(\rm IS) = -61.6$ and -13.2 km s^{-1} as well as a circumstellar component with $V(\rm CS) = -41.0$ km s^{-1} whose position corresponds to the velocity inferred from C_2 features. The presence of the interstellar component with $V_r = -61.6$ km s^{-1} in the spectrum allows $d = 2.5$ kpc to be considered as a lower limit for the distance to the star. A splitting of the profiles for strong absorptions of ionized metals (Y II, Ba II, La II, Si II) attributable to the presence of a short-wavelength component originating in the circumstellar envelope has been detected in the optical spectrum of IRAS 23304+6347 for the first time.

DOI: 10.1134/S1063773715020024

Keywords: *stars, evolution, post-AGB stars, envelopes, spectra.*

1. INTRODUCTION

In this paper, we continue to investigate the optical spectra of Galactic infrared (IR) sources identified with highly evolved stars at the short-lived post-asymptotic-giant-branch (post-AGB) evolutionary stage, at which intermediate-mass ($3-8\,M_\odot$) stars rapidly pass into the planetary-nebula phase. Kwok (1993) pointed out the main signatures of protoplanetary nebulae (PPNe): high-absolute-luminosity stars with large IR excesses, evidence of mass loss, and a detached expanding gas–dust envelope.

Our comprehensive studies of supergiants with large IR excesses have led to the determination (or refinement) of their evolutionary status. One of the results of our spectroscopy for a sample of high-luminosity stars, PPN candidates, is the conclusion reached by Klochkova (2012) about the inhomogeneity of this sample. Apart from PPNe, the sample produced on the basis of IR photometry and low-resolution spectroscopy includes young pre-main-sequence stars, high-luminosity stars of various types, from low-mass semiregular variables to hypergiants.

The fact that PPNe belong to the post-AGB stage makes them extremely interesting both in investigating the final evolutionary stages of intermediate-mass stars and in studying the chemical evolution of stars and galaxies as a whole. The atmospheres of stars at such an advanced evolutionary stage have chemical peculiarities attributable to the successive change of energy-releasing nuclear reactions accompanied by a change in the structure and chemical composition of the stellar envelope, the mixing of matter, and the dredge-up of nuclear-reaction products to the surface layers of the atmosphere. A small homogeneous subgroup of PPNe with evolutionary overabundances of carbon and heavy metals found in the atmospheres of their central stars has been identified over the last two decades during the spectroscopy of a sample of PPN candidates at the world's largest telescopes (Klochkova 1995, 2013; Začs et al. 1995; Reddy et al. 1997, 1999, 2002; Klochkova et al. 1999, 2000a, 2000b; van Winckel and Reyniers 2000; Kipper and Klochkova 2006). The circumstellar envelopes of these objects have a complex morphology and are

*E-mail: valenta@sao.ru

generally enriched in carbon, which manifests itself in the presence of carbon-containing C_2, C_3, CN, CO, etc. molecular bands in their IR, radio, and optical spectra. These PPNe belong to those few objects whose spectra exhibit the 21-μm envelope emission band (Kwok et al. 1999, Hrivnak et al. 2009). Despite an active search for appropriate chemical agents, there is no ultimate identification of this extremely rarely observed feature at present. However, its presence in the spectra of PPNe with carbon-enriched envelopes suggests that this emission may be due to the presence of a complex carbon-based molecule in the envelope (for details and references, see Hrivnak et al. 2009).

A circumstellar gas–dust envelope manifests itself in peculiarities of the radio, IR, and optical spectra of post-AGB supergiants. The optical spectra of PPNe differ from those of classical massive supergiants by the presence of molecular bands superimposed on the spectrum of an F–G supergiant and by the anomalous behavior of the profiles for selected spectral features. These can be the complex emission–absorption profiles of H I, Na I, and He I lines, the profiles of strong absorptions distorted by emissions or splitting, and metal emissions. All these peculiarities are often variable. The manifestations of the circumstellar envelope in the optical spectra of PPNe are considered in more detail in Klochkova (2014). The previous results of our spectroscopy for PPNe with the 6-m BTA telescope were published in a series of original papers and are summarized in the reviews by Klochkova (1997, 2012, 2014). In this paper, we present new results of our high-resolution spectroscopy for the post-AGB star identified with the IR source IRAS 23304+6147 (below referred to as IRAS 23304). The central star of IRAS 23304 is a rather faint ($B = 15\overset{m}{.}52$, $V = 13\overset{m}{.}15$) supergiant of spectral type G2 Ia lying near the Galactic plane ($b = 0.58°$). According to the high-spatial-resolution Hubble Space Telescope observations by Sahai et al. (2007), the circumstellar envelope in this system has a complex structure including a multipole and an extended halo with arc-shaped features.

The first study of the optical spectrum for the central star of IRAS 23304 belonging to the group of stars with atmospheres enriched in carbon and heavy metals and the calculations of elemental abundances in its atmosphere were performed by Klochkova et al. (2000a). In this paper, we determined the main parameters of the star: its effective temperature $T_{\rm eff} = 5900$ K, surface gravity $\log g = 0.0$, reduced metallicity relative to the Sun $[{\rm Fe/H}] = -0.61$, and the abundances of 25 other chemical elements. van Winckel and Reyniers (2000) found similar chemical peculiarities based on a higher-resolution spectrum. However, in both publications aimed mainly at studying the fundamental parameters of the star and the chemical composition of its atmosphere, little attention was given to the peculiarities of its spectrum, the pattern of radial velocities, and their variability with time. In this paper, the peculiarities of the optical spectrum for the central star of IRAS 23304 and their variability are considered in more detail.

Our observational data are briefly described in Section 2. The peculiarities of the profiles for the Hα, Na I doublet, metal lines detected from high-resolution spectra and molecular bands as well as the data on the velocity field in the supergiant's atmosphere and envelope are considered in Section 3. Our main conclusions are presented in Section 4.

2. OBSERVATIONAL DATA

In this paper, we use the spectra taken at the Nasmyth focus with the NES echelle spectrograph (Panchuk et al. 2007, 2009) on October 12, 2013. In combination with an image slicer (Panchuk et al. 2003), the NES spectrograph provides a spectral resolution $R \approx 60\,000$. A 2048×4096-pixel CCD array has been used at the NES spectrograph since 2011, which has allowed the recorded spectral range to be extended considerably. In addition, for comparison, we used the star's spectra taken with the PFES echelle spectrograph (Panchuk et al. 1998) at the prime focus of the BTA telescope with a resolution $R \approx 15\,000$ during several observational sets in 1997.

The details of our spectrophotometric and positional measurements of the spectra were described in previously published papers; the corresponding references to them are given in Klochkova (2014). Note that applying the image slicer required a significant modification of the standard ECHELLE context of the MIDAS software package. The data were extracted from two-dimensional echelle spectra with the software package described in Yushkin and Klochkov (2005). The DECH code (Galazutdinova 1992), which allows, in particular, the radial velocities to be measured from individual features of complex lines typical for the spectra of the program stars, was used to reduce the extracted spectra.

3. PECULIARITIES OF THE OPTICAL SPECTRUM AND THE VELOCITY FIELD FOR THE STAR

It follows from our spectroscopy for the sample of PPNe that the following main types of spectral features are observed in their optical spectra: (1) low- or moderate-intensity metal absorptions whose symmetric profiles have no apparent distortions; (2) complex neutral hydrogen line profiles changing with time and including absorption and emission components;

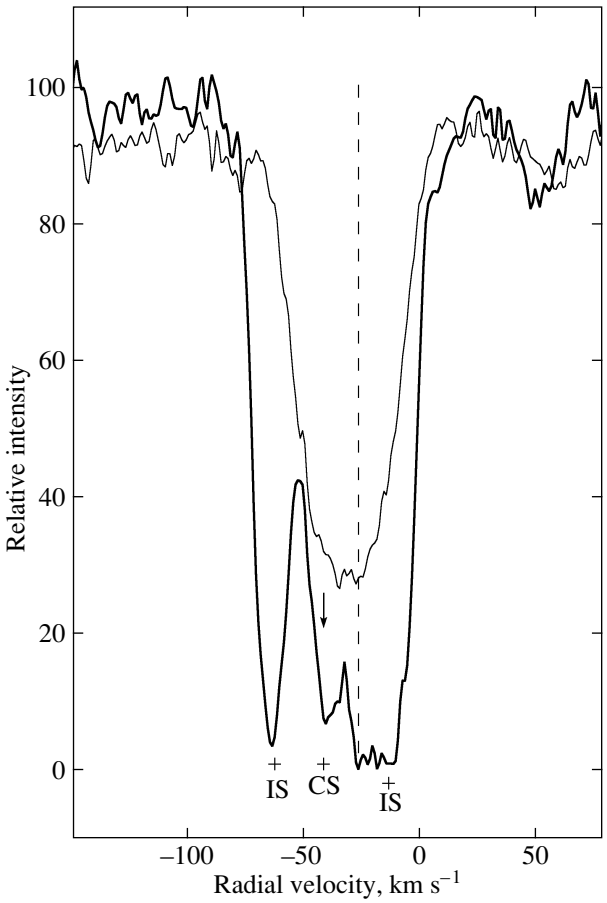

Fig. 1. Hα (thin curve) and Na I D2 (thick curve) line profiles in the spectrum of IRAS 23304. The arrow marks the envelope velocity inferred from the the C_2 Swan band, $V_r(\mathrm{CS}) = -41$ km s^{-1}. The crosses plot the positions of two interstellar (IS) and circumstellar (CS) components of the Na I D2 line. The vertical dashed line indicates the systemic velocity. Here and in Fig. 2, the intensity of the normalized continuum along the vertical axis is taken as 100.

(3) the strongest metal absorptions with a low lower-level excitation potential, their variable profiles are often distorted by envelope features causing an asymmetry of the profile or its splitting into components; (4) absorption or emission bands of molecules, mostly carbon-containing ones; (5) envelope components of the Na I and K I resonance lines; and (6) narrow permitted or forbidden emission lines of metals originating in the envelopes. The main difference between the spectra of PPNe and massive supergiants is the presence of features of types 2–6.

All the main peculiarities of the optical spectra for PPNe are contained in the spectra of the post-AGB star HD 56126. The latter may be considered by the combination of observed properties (a typical double-humped spectral energy distribution, an F-supergiant spectrum with a variable absorption–emission Hα line profile, the presence of C_2 Swan molecular bands in the optical spectrum originating in an outflowing extended envelope, large overabundances of carbon and heavy metals synthesized during the star's evolution through the s-process and dredged up to the surface layers of the atmosphere through mixing) as a canonical post-AGB star. As follows from Fig. 2 in the spectral atlas (Klochkova et al. 2007) based on a long-term monitoring of HD 56126 with BTA, the Hα profile in its spectrum took all of the varieties listed above: an asymmetric core, a direct or inverse P Cyg profile, and a profile with two emissions in the wings.

In the subgroup of PPNe with the 21-μm emission feature, the central star of the IR source IRAS 23304 belongs to the coolest ones (its spectral type is G2 Ia), with the effective temperature $T_{\mathrm{eff}} = 5900$ K. The temperatures in the central stars of IRAS 22272+5435 (G5 Ia) and IRAS 20000+3239 (G8 Ia) are even lower: $T_{\mathrm{eff}} = 5650$ (Klochkova et al. 2009) and 5000 K (Klochkova and Kipper 2006), respectively.

Spectroscopic data and heliocentric radial velocities V_r, km s^{-1}, measured from various spectral features. The number of lines used to determine the mean velocity is given in parentheses

Date	$\Delta\lambda$, Å	V_r, km s^{-1}					
		absorptions (297)	Hβ	Hα	C_2 (24)	Na I (2)	DIB (4)
Oct. 12, 2013	4500–6980	-25.7 ± 0.2	-27.8	-26.6		-26.0	
						-61.6	
					-41.3 ± 0.2	-41.0	
						-13.2	-14.0 ± 1.3

3.1. The Hα Line

The Hα line in the PPN spectra has complex (a combination of emission and absorption components), time-varying profiles of various types: with an asymmetric core, P Cyg or inverse P Cyg ones, and with two emission components in the wings. The presence of an emission in the Hα line points to a high mass loss rate and is one of the criteria for searching and identifying PPNe. The Hα profile in the spectrum of IRAS 23304 is also subjected to significant changes: in Fig. 1 from Klochkova et al. (2000a), a strong emission is superimposed on the short-wavelength wing of the absorption profile typical of G supergiants. The profile in the spectrum taken in 2013 and presented in Fig. 1 in "relative intensity–V_r" coordinates has an absorption core of the same depth as that in the 1997 spectrum, but it contains no peculiarities.

3.2. Molecular Features

In their paper devoted to investigating the molecular component of the PPN spectra, Bakker et al. (1997) point out the presence of C_2 bands for the source IRAS 23304 whose positions in the spectrum correspond to the circumstellar envelope velocity $V_r(\mathrm{CS}) = -39.7$ km s^{-1}, which leads to the envelope expansion velocity $V_{\mathrm{exp}} = 13.9$ km s^{-1}. The observations of two envelope CO bands give the envelope expansion velocity $V_{\mathrm{exp}} = 9.2$ and 10.3 km s^{-1} (Hrivnak et al. 2005). We emphasize that Bakker et al. (1997) pointed out the presence of Swan bands in the form of absorption features. The (0; 0) 5165 Å absorption band was also recorded in our 2000 and 2013 spectra. However, the intensity in the head of the (0; 1) 5635 Å band in both spectra exceeds appreciably the local continuum level, i.e., we detected a complex absorption–emission profile of the (0; 1) 5635 Å band.

The table gives the radial velocity $V_r(\mathrm{C_2}) = -41.3 \pm 0.2$ km s^{-1} that we measured from the positions of 24 rotational lines of the Swan 5165 Å band in the 2013 spectrum. Taking into account the systemic velocity $V_{\mathrm{sys}}(\mathrm{CO}) = -25.8$ km s^{-1} from Woodsworth et al. (1990), we obtain the envelope expansion velocity $V_{\mathrm{exp}} = 15.5$ km s^{-1}. A velocity $V_r(\mathrm{C_2}) \approx -50$ km s^{-1} was derived in Klochkova et al. (2000a) from the positions of the band heads because of the lower spectral resolution. When an asymmetric head with a shade of violet is convolved with a low spectral resolution, the position of the head is shifted to a short-wavelength velocity, which explains the difference in the results of the measurements in the 1997 and 2013 spectra.

3.3. The Na I Doublet Resonance Lines and Diffuse Bands

The heliocentric radial velocities for the main components of the Na I D lines presented in Fig. 1 are -61.6, -41.0, -26.0, and -13.2 km s^{-1} (see the table). Here, it should be noted that the velocities for these components differ from those in our previous publication (Klochkova et al. 2000a). The moderate resolution ($R = 15\,000$) in the spectra used in this paper was insufficient for the identification of individual components in the complex Na I D line profile. The component of the Na I D doublet lines whose position corresponds to the velocity $V_r = -26.0$ km s^{-1} originates in the stellar atmosphere, because its position agrees with the positions of the overwhelming majority of atmospheric absorptions in the spectrum of the optical counterpart of IRAS 23304. The longer-wavelength component, $V_r = -13.2$ km s^{-1}, is interstellar and originates in the Local arm of the

Galaxy. The shortest-wavelength component, $V_r = -61.6$ km s^{-1}, of the Na I doublet is also interstellar; it originates in the interstellar medium of the Perseus arm. The presence of an analogous interstellar component with $V_r \approx -63$ km s^{-1} in the spectra of the B stars HD 4841, HD 4694, and Hiltner 62, whose positions in the Galaxy are close to the longitude of IRAS 23304, serves as an argument for this. The spectra of these stars, members of the Cas OB7 association, were studied by Miroshnichenko et al. (2009). The presence of the component with $V_r = -61.6$ km s^{-1} allows us to consider the distance to the Cas OB7 association $d = 2.5$ kpc from Cazzolato and Pineault (2003) as a lower limit for the distance to IRAS 23304.

Regarding the component of the Na I D lines with $V_r = -41.0$ km s^{-1}, it is natural to assume that it originates in the expanding circumstellar envelope of IRAS 23304, where the Swan bands are also formed (the close radial velocity $V_r(\mathrm{CS}) = -39.7$ km s^{-1} corresponds to their positions). Thus, we obtain an envelope expansion velocity $V_{\mathrm{exp}} \approx 13$ km s^{-1} typical for PPNe (Loup et al. 1993; Klochkova 2014).

According to the results of Miroshnichenko et al. (2009), there are diffuse interstellar bands (DIBs) with velocities in the range from -11 to -14 km s^{-1} in the spectra of the hot stars HD 4841, HD 4694, and Hiltner 62 mentioned above. It is also natural to expect the presence of DIBs in the spectra of the optical counterpart of IRAS 23304. Luna et al. (2008) provide their measurements of the positions of DIBs that have a very large spread of V_r in the spectrum of IRAS 23304, from -26 to $+5$ km s^{-1}. We measured the positions of five absorptions that could be identified with the 5797, 6196, 6203, 6207, and 6613 Å DIBs. The mean velocity for them is $V_r(\mathrm{DIBs}) = -15$ km s^{-1}. If, however, we discard the 6613 Å band blended in the spectrum of the program supergiant by a strong Y II line, then we obtain a mean velocity $V_r(\mathrm{DIBs}) = -14.0 \pm 1.3$ km s^{-1} close to $V_r = -13.2$ km s^{-1} inferred from the longest-wavelength component of the Na I D lines. For a more definite conclusion about the positions of DIBs in the spectrum of a cool supergiant, it is necessary to have observational data with an ultrahigh spectral resolution, $R \geq 100\,000$.

3.4. Asymmetry of the Profiles for Strong Absorptions of Ionized Metals

Thanks to their high spectral resolution ($R = 60\,000$), the 2013 observations allowed us to detect one more, previously unknown peculiarity of the optical spectrum for IRAS 23304, complex (asymmetric or split) profiles of the strongest metal absorptions. This peculiarity is clearly seen in Fig. 2, where the Ba II λ 6141, 6496 Å, Y II 5200 Å, La II 6390 Å, and Si II 6347 Å line profiles are presented. The Ba II absorptions in the spectrum of IRAS 23304 are enhanced to such an extent that their equivalent widths W_λ are comparable to those for the neutral hydrogen lines: $W_\lambda(6141) = 0.76$ Å, $W_\lambda(\mathrm{H}\alpha) = 0.84$ Å.

Let us consider the detected effect in slightly more detail using the selected lines presented in Fig. 2 in "relative intensity–V_r" coordinates as an example. As can be seen from Fig. 2 and the data in the table, the profiles of these lines include a component whose position coincides with the positions of symmetric absorptions in the spectrum and a short-wavelength component whose position corresponds to the velocity inferred from the C_2 Swan band. The proposed interpretation of the complex profile is confirmed by our comparison of the line profiles in Figs. 1 and 2. The position of the short-wavelength component also coincides with the position of the circumstellar component in the Na D1 profile.

Thus, it can be asserted that, apart from the photospheric component, the complex Ba II line profile contains a component originating in the circumstellar envelope, suggesting an efficient dredge-up of the heavy metals produced during the preceding evolution of this star into the envelope. The separation between the atmospheric and circumstellar line components is about 15 km s^{-1}. All the lines of heavy-metal ions (Ba II, Y II, La II) in which a profile asymmetry was detected are distinguished by a low lower-level excitation potential, $\chi_{\mathrm{low}} < 1$ eV. As the spectral resolution is reduced, the intensity of the envelope components will be added to the intensity of the components originating in the atmosphere, which will lead to an overestimation of the heavy-element abundances determined from strong absorptions. The abundances determined from low- and moderate-intensity lines will be more realistic.

A complex profile for the absorptions of heavy-metal ions that, apart from the photospheric component, also contains the circumstellar one was found previously in the spectra of the related post-AGB stars V354 Lac = IRAS 22272+5435 (Klochkova 2009), V448 Lac = IRAS 22223+4327 (Klochkova et al. 2010), and V5112 Sgr = IRAS 19500−1709 (Klochkova 2013). The envelope effect in the spectrum of the high-latitude supergiant V5112 Sgr, which enters the group of PPNe with an atmosphere enriched in carbon and heavy metals and its IR spectrum contains the 21-μm emission feature, is of greatest interest. An asymmetry and splitting of strong absorptions with a low lower-level excitation potential were detected in the spectra of V5112 Sgr taken with the NES echelle spectrograph at BTA

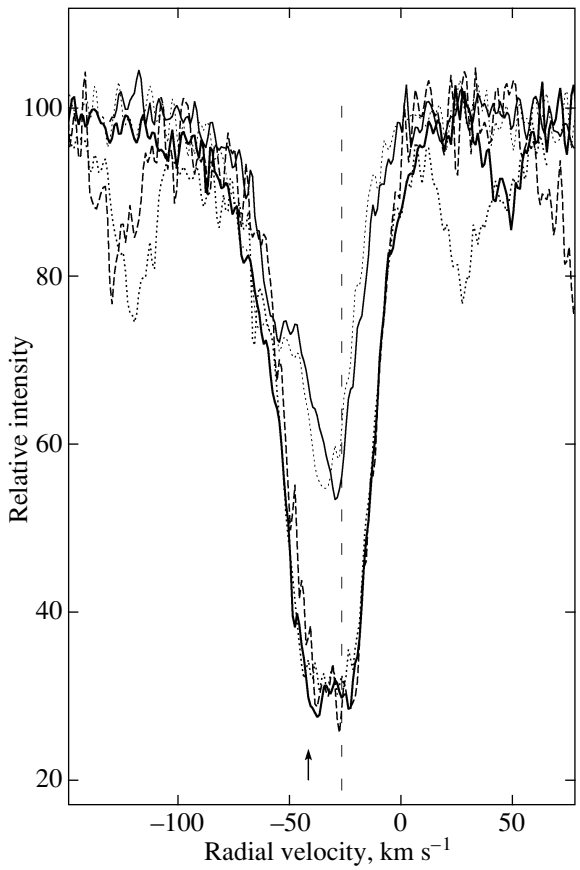

Fig. 2. Profiles of selected lines in the optical spectrum for the central star of IRAS 23304. The lower group of lines: Ba II 6141 (thick solid curve), Ba II 6496 (dotted curve), and Y II 5200 (dashed curve). The upper group: La II 6390 (thin solid curve) and Si II 6347 (dotted curve). The arrow marks the envelope velocity $V_r(\mathrm{CS}) = -41$ km s^{-1} inferred from the C_2 Swan band. The vertical dashed line indicates the systemic velocity.

(Klochkova 2013). The effect is maximal for the Ba II lines whose profile is split into three components. The shape of the profiles for the split lines and their positions change with time. Our analysis of the velocity field led us to conclude that both short-wavelength components of the split absorptions originate in the structured circumstellar envelope of V5112 Sgr.

We emphasize that the strong Si II 6347 and 6371 Å lines in the spectrum of the optical counterpart of IRAS 23304 are also asymmetric (Fig. 2). Apart from the photospheric component, both these lines include a weak short-wavelength component whose position points to its formation in the star's gaseous envelope. This peculiarity of the Si II lines is consistent with a significant silicon overabundance in the stellar atmosphere (Klochkova et al. 2000a; van Winckel and Reyniers 2000). Thus, for the first time we have detected the dredge-up of not only s-process elements but also silicon into the envelope. The synthesis of silicon is possible through the capture of protons by heavier nuclei in the hot layers of the convective envelope in massive AGB stars with initial masses higher than 4 $M_\odot$. A description of this so-called "hot bottom burning" (HBB) and the necessary references are available in Ventura et al. (2011) devoted to the synthesis of Mg, Al, and Si through HBB.

3.5. The Velocity Field in the Atmosphere and Envelope

The heliocentric radial velocity of IRAS 23304 that we measured from a large set of visually symmetric absorptions without any clear bands is $V_r(\mathrm{abs}) = -25.7 \pm 0.2$ km s^{-1}. First, this velocity coincides with the systemic velocity $V_{\mathrm{sys}}(\mathrm{CO}) = -25.8$ km s^{-1} inferred from the radio CO observations performed by Woodsworth et al. (1990) for a sample of PPNe with the 21-μm band. Second, the velocity we found agrees well with the velocity estimated from absorptions for two times of observations of IRAS 23304 in 1994 ($V_r = -26$, -26 km s^{-1} from the data of van Winckel and Reyniers (2000)) and three times of its observations in 1997 ($V_r = -23.4$, -24.9,

-25.3 km s^{-1} from the measurements by Klochkova et al. (2000a)). This constancy of the velocity leads us to the preliminary conclusion about the absence of pulsations and signatures of binarity in the system. However, it should be noted that Hrivnak et al. (2010) revealed a weak brightness variability of the object with an amplitude of about $0\overset{m}{.}2$ and a period $P \approx 85$ days as a result of their long-term photometric monitoring of IRAS 23304. The parameters of the brightness and color variability in IRAS 23304 derived by Hrivnak et al. (2010) are typical for PPNe with a temperature close to that of IRAS 23304. As regards the V_r variability, the weak velocity variability from the available, so far scarce data distinguishes this object among the remaining PPNe with enriched atmospheres. Having studied the variability for seven such PPNe, Hrivnak et al. (2011) found a pulsational V_r variability with amplitudes of $\sim$10 km s^{-1}.

It is pertinent to dwell on the methodological aspects of studying the velocity field in the atmospheres of PPNe. The overwhelming majority of the radial velocities used by Hrivnak et al. (2013) were obtained with CORAVEL-type spectrometers. For definiteness, consider the results obtained by these authors for V354 Lac (IRAS 22272+5435). The measurements were performed predominantly by various cross-correlation techniques. A fundamental shortcoming of the single-channel methods is a mismatch between the scales of the spectrum and the shifted spectral mask arising at any change in the star's radial velocity. In the period 1991–1995, Hrivnak et al. (2013) used the DAO cross-correlation photometer (Fletcher et al. 1982; McClure et al. 1985). The above mismatch between the scales was partly compensated for by a special design of the mask (a system of tall slits in the range 4000–4600 Å, with a slope changing with distance from the mask center) and a special law of mask motion (at 45° to the spectrum axis).

In their description of the DAO correlation photometer, Fletcher et al. (1982) point out a systematic zero-point drift for the radial velocities (1 km s^{-1} in 2 h), which they managed to reduce by half, to 0.5 km s^{-1}, by frequent zero-point calibration based on a comparison spectrum. Since the correlation photometer at the coudé focus of the DAO 1.2-m telescope is not subjected to any mechanical deformations, the above zero-point drift for the radial velocities is completely determined by the filling of the spectrograph aperture, variable with the object's horizontal coordinates.

The radial-velocity measurements in the period 2007–2011 performed from the spectra taken with a CCD array in the range 4350–4500 Å are free from the mismatch of the scales, because the mask is no longer mechanical but digital; besides, the wavelength range is shorter by four times. The longer the spectrum interval intercepted by the mask, the more pronounced the mismatch between the mask and spectrum scales. This problem was solved by T. Walraven and J. Walraven (1972) by using short spectral orders, i.e., by applying echelle correlation photometers.

The third series of radial-velocity measurements for IRAS 22272+5435 was performed with an echelle correlation photometer whose design, in fact, copies the photometer of Tokovinin (1987). Upgren et al. (2002) provided the errors calculated from the "cross-correlation dip area–radial velocity error" relationship taken from Jasniewicz and Mayor (1988) for this photometer based on 153 individual measurements performed for 149 stars. Excluding the errors of more than 1.1 km s^{-1}, we obtained a mean error of 0.83 km s^{-1} for 142 stars from Table 1 in Upgren et al. (2002). For Tokovinin's correlation photometer, the error due to construction flexure reaches 0.6 km s^{-1}, but it can be reduced to 0.1 km s^{-1} by orienting the slit parallel to the vertical circle (Tokovinin 1987). However, the errors due to atmospheric dispersion shifting the centers of the star's monochromatic images across the slit increase in this case. The angular width of the correlation-photometer slit is $\sim$1 arcsec; the centers of the monochromatic images for the extreme wavelengths of the simultaneously recorded range (4000–6000 Å) will be separated virtually by the same amount at a zenith distance of 45°. The estimate was obtained from the tables of differential refraction calculated by Filippenko (1982) for the altitude $h = 2$ km. The differential refraction effect for the Moletai Observatory ($h = 0.2$ km) is more pronounced.

Let us estimate the radial-velocity error due to inaccurate centering of the star on the slit. For an autocollimation photometer, the scales on the entrance slit and on the mask are identical. For $\lambda = 4400$ Å, a shift of the spectrum by 0.0074 mm corresponds to a Doppler shift by 1 km s^{-1} (Tokovinin 1987). This means that a radial-velocity measurement error of 1 km s^{-1} can be obtained at an error in centering the star on the slit of 0.01 arcsec. An optical element "tangling" the rays along the slit width was used as the slit in Tokovinin's photometer. The slit width in the photometer used by Hrivnak et al. (2013) is 0.11 mm (Upgren et al. 2002). The standard star and the program star cannot be unambiguously set on the slit with an accuracy better than 0.1 arcsec even in the presence of an autoguider.

On the whole, it can be asserted that the instrumental effects of the single-channel correlation techniques limit the accuracy of V_r measurements

at 0.8 km s^{-1}. This value should be kept in mind when interpreting the peculiarities of the radial-velocity curve for IRAS 22272+5435 provided by Začs et al. (2009). Recall that periodic radial-velocity oscillations with a semi-amplitude of 3.1 km s^{-1} were detected in this paper, with the overall scatter of individual measurements from the mean heliocentric velocity reaching ± 5 km s^{-1}. Note that we obtain an accuracy of $\approx$0.8 km s^{-1} typical for cross-correlation techniques from the spectra when measuring the position of a single line (Klochkova et al. 2010). In the spectra of F supergiants, the accuracy of V_r from an ensemble of several hundred symmetric absorptions is an order of magnitude better.

In addition, in the case of a correlation technique of V_r measurements, the possible peculiarities of the profiles for strong lines attributable to a complex pattern of the velocity field in the atmospheres of these stars and the influence of the circumstellar envelope on the profiles are disregarded. Based on the spectra taken with BTA in a wide wavelength range, we found an asymmetry and splitting of the profiles for low-excitation lines in the spectra of the post-AGB stars V5112 Sgr (Klochkova 2013), V354 Lac (Klochkova 2009), and V448 Lac (Klochkova et al. 2010). This is primarily observed in the Ba II, Y II, and La II resonance absorption lines. A temporal variability of the profiles for the above lines was revealed. The set of peculiarities of these profiles can be explained by a superposition of spectral features: absorptions originating in the stellar atmosphere and an envelope emission. The anomalies of the profiles and their variability can affect significantly the conclusions about the pulsation properties. For instance, for V448 Lac, Klochkova et al. (2010) detected differential line shifts reaching 8 km s^{-1} and a very low pulsation amplitude $\Delta V_r \approx 1-2$ km s^{-1}, while Hrivnak et al. (2013) found an amplitude exceeding this value manyfold.

The large spread of V_r for close times of observations of V354 Lac and V448 Lac (Hrivnak et al. 2013) at a more regular brightness variation in the star can probably be explained by the neglect of both instrumental and these subtle kinematic effects. The amplitude of the differential shifts in the atmosphere of the post-AGB star HD 56126 is even more significant (Klochkova and Chentsov 2007): they reach 15 km s^{-1} for metal lines. Thus, apart from the pulsational variability with time, the pattern of V_r variations in the case of PPNe can also be complicated by differential motions in the extended atmospheres of the program objects. A detailed analysis of V_r based on high spectral- and time-resolution spectra for the selected, brightest PPNe allows the differences in the behavior of V_r determined from lines with different degrees of excitation originating at different depths in the stellar atmosphere to be detected.

4. CONCLUSIONS

Based on our high-spectral-resolution observations performed with the echelle spectrograph of the 6-m telescope, we studied the peculiarities of the spectrum and the details of the velocity field in the atmosphere and envelope of a faint supergiant, the central star of the IR source IRAS 23304+6347. Our comparison of the radial velocity $V_r = -25.7$ km s^{-1} inferred from numerous low- and moderate-intensity symmetric absorptions with previously published results points to the absence of significant variations in the velocity and its coincidence with the systemic velocity deduced from radio data.

Based on our measurements of the positions for 24 rotational lines of the C_2 Swan $(0;0)$ λ 5165 Å band, we determined the envelope expansion velocity $V_{\rm exp} = 15.5$ km s^{-1}, typical for post-AGB stars. A complex emission–absorption profile was detected for the Swan $(0;1)$ 5635 Å band.

Our analysis of the multicomponent Na I D doublet line profile revealed interstellar components with velocities $V(\mathrm{IS}) = -61.6$ and -13.2 km s^{-1} as well a circumstellar component with $V(\mathrm{CS}) = -41.0$ km s^{-1} whose position corresponds to the velocity inferred from C_2 features. The shortest-wavelength component ($V_r = -61.6$ km s^{-1}) of the Na I D lines originates in the interstellar medium of the Perseus arm. Its presence allows $d = 2.5$ kpc to be considered as a low limit for the distance to IRAS 23304.

Based on four features identified with diffuse interstellar bands (DIBs), we found the mean velocity $V_r(\mathrm{DIBs}) = -14.0 \pm 1.3$ km s^{-1} close to $V_r = -13.2$ km s^{-1} inferred from the long-wavelength interstellar component of the Na I D lines.

An asymmetry of the profiles for strong absorptions of ionized metals (Y II, Ba II, La II, Si II) attributable to the presence of a short-wavelength component originating in the circumstellar envelope in these lines has been detected in the optical spectrum of IRAS 23304+6347 for the first time. The overabundance of silicon whose synthesis is possible through the hot bottom burning process in the hot layers of the convective envelope in massive AGB stars suggests that the star being investigated belongs to stars with initial masses higher than 4 $M_\odot$.

ACKNOWLEDGMENTS

This work was supported by the Russian Foundation for Basic Research (project no. 14-02-00291a). We used the SIMBAD and ADS astronomical databases.

REFERENCES

1. E. J. Bakker, E. F. van Dishoeck, L. B. F. M. Waters, and T. Schoenmaker, Astron. Astrophys. **323**, 469 (1997).
2. F. Cazzolato and S. Pineault, Astron. J. **125**, 2050 (2003).
3. A. V. Filippenko, Publ. Astron. Soc. Pacif. **94**, 715 (1982).
4. J. M. Fletcher, H. C. Harris, R. D. McClure, and C. D. Scarfe, Publ. Astron. Soc. Pacif. **94**, 1017 (1982).
5. G. A. Galazutdinov, Preprint Spets. Astrofiz. Observ. RAN, No. 92 (1992).
6. B. J. Hrivnak and J. H. Bieging, Astrophys. J. **624**, 331 (2005).
7. B. J. Hrivnak, W. Lu, R. E. Maupin, and B. D. Spitzbart, Astrophys. J. **709**, 1042 (2010).
8. B. J. Hrivnak, W. Lu, J. Sperauskas, H. van Winckel, D. Bohlender, and L. Začs, Astrophys. J. **766**, 116 (2013).
9. B. J. Hrivnak, K. Volk, and S. Kwok, Astrophys. J. **694**, 1147 (2009).
10. G. Jasniewicz and M. Mayor, Astron. Astrophys. **203**, 329 (1988).
11. V. G. Klochkova, Mon. Not. R. Astron. Soc. **272**, 710 (1995).
12. V. G. Klochkova, Astrophys. Bull. **44**, 5 (1997).
13. V. G. Klochkova, Astron. Lett. **35**, 457 (2009).
14. V. G. Klochkova, Astrophys. Bull. **67**, 385 (2012).
15. V. G. Klochkova, Astron. Lett. **39**, 765 (2013).
16. V. G. Klochkova, Astrophys. Bull. **69**, 279 (2014).
17. V. G. Klochkova and E. L. Chentsov, Astron. Rep. **51**, 994 (2007).
18. V. G. Klochkova and T. Kipper, Baltic Astron. **15**, 395 (2006).
19. V. G. Klochkova, R. Szczerba, V. E. Panchuk, and K. Volk, Astron. Astrophys. **345**, 905 (1999).
20. V. G. Klochkova, R. Szczerba, and V. E. Panchuk, Astron. Lett. **26**, 88 (2000a).
21. V. G. Klochkova, R. Szczerba, and V. E. Panchuk, Astron. Lett. **26**, 439 (2000b).
22. V. G. Klochkova, E. L. Chentsov, N. S. Tavolganskaya, and M. V. Shapovalov, Astrophys. Bull. **62**, 162 (2007).
23. V. G. Klochkova, V. E. Panchuk, and N. S. Tavolganskaya, Astrophys. Bull. **64**, 155 (2009).
24. V. G. Klochkova, V. E. Panchuk, and N. S. Tavolganskaya, Astron. Rep. **54**, 234 (2010).
25. S. Kwok, Ann. Rev. Astron. Astrophys. **31**, 63 (1993).
26. S. Kwok, K. Volk, and B. J. Hrivnak, IAU Symp., No. 191, 297 (1999).
27. C. Loup, T. Forveille, A. Omont, and J. F. Paul, Astron. Astrophys. Suppl. Ser. **99**, 291 (1993).
28. R. D. McClure, J. M. Fletcher, W. A. Grundman, and E. H. Richardson, IAU Coll., No. 88, 49 (1985).
29. A. S. Miroshnichenko, E. L. Chentsov, V. G. Klochkova, S. V. Zharikov, K. N. Grankin, A. V. Kusakin, T. L. Gandet, G. Klingenberg, et al., Astrophys. J. **700**, 209 (2009).
30. V. Panchuk, V. Klochkova, M. Yushkin, and I. Najdenov, in *Proceedings of the Joint Discussion No. 4 during the IAU General Assembly of 2006,* Ed. by A. I. Gomez de Castro and M. A. Barstow (Editorial Complutense, Madrid, 2007), p. 179.
31. V. E. Panchuk, V. G. Klochkova, M. V. Yushkin, and I. D. Naidenov, J. Opt. Technol. **76**, 87 (2009).
32. V. E. Panchuk, M. V. Yushkin, and I. D. Naidenov, Preprint Spets. Astrofiz. Observ. RAN No. 179 (2003).
33. B. E. Reddy, M. Parthasarathy, G. Gonzalez, and E. J. Bakker, Astron. Astrophys. **328**, 331 (1997).
34. B. E. Reddy, E. J. Bakker, and B. J. Hrivnak, Astrophys. J. **524**, 831 (1999).
35. B. E. Reddy, D. L. Lambert, G. Gonzalez, and D. Yong, Astrophys. J. **564**, 482 (2002).
36. R. Sahai, M. Morris, C. Sánchez Contreras, and M. Claussen, Astron. J. **134**, 2200 (2007).
37. A. A. Tokovinin, Sov. Astron. **31**, 98 (1987).
38. A. R. Upgren, J. Sperauskas, and R. P. Boyle, Baltic Astron. **11**, 91 (2002).
39. P. Ventura, R. Carini, and F. D. D'Antona, Mon. Not. R. Astron. Soc. **415**, 3865 (2011).
40. T. Walraven and J. H. Walraven, *Auxiliary Instrumentation for Large Telescopes,* Ed. by S. Lautsen and A. Reiz (ESO, 1972), p. 175.
41. H. van Winckel and M. Reyniers, Astron. Astrophys. **354**, 135 (2000).
42. A. W. Woodsworth, S. Kwok, and S. J. Chan, Astron. Astrophys. **228**, 503 (1990).
43. M. V. Yushkin and V. G. Klochkova, Preprint Spets. Astrofiz. Observ. RAN, No. 206 (2005).
44. L. Začs, V. G. Klochkova, and V. E. Panchuk, Mon. Not. R. Astron. Soc. **275**, 764 (1995).
45. L. Začs, J. Sperauskas, F. A. Musaev, O. Smirnova, T. C. Yang, W. P. Chen, and M. Schmidt, Astrophys. J. **695**, L203 (2009).

Translated by V. Astakhov